Article

Experimental Assessment of a Centralised Controller for High-RES Active Distribution Networks

Francisco de Paula García-López, Manuel Barragán-Villarejo, Alejandro Marano-Marcolini, José María Maza-Ortega and José Luis Martínez-Ramos

Department of Electrical Engineering, Universidad de Sevilla, Camino de los Descubrimientos s/n, 41092, Seville, Spain

* Correspondence: manuelbarragan@us.es

Abstract: This paper assesses the behaviour of active distribution networks with high penetration of renewable energy sources when the control is performed in a centralised manner. The control assets are the on-load tap changers of transformers at the primary substation, the reactive power injections of the renewable energy sources and the active and reactive power exchanged between adjacent feeders when they are interconnected through a DC link. A scaled-down distribution network is used as testbed to emulate the behaviour of an active distribution system with massive penetration of renewable energy resources. The laboratory testbed involves hardware devices, real-time control, and communication infrastructure. Several key performance indices are adopted to assess the effects of the different control actions on the system operation. The experimental results demonstrate that the combination of control actions enables the optimal integration of a massive penetration of renewable energy.

Keywords: active distribution network; laboratory testbed; renewable energy sources; DC link; centralised control.

1. Introduction

Massive penetration of renewable energy sources (RES) is unstoppable nowadays because of the need of reducing the dependency of fossil fuels. This new technology of generation assets is being deployed in small units within medium voltage (MV) and low voltage (LV) distribution systems, the so-called distributed generation, in contrast to the conventional connection of large-scale power plants to HV systems. The drivers behind this change in the generation paradigm are threefold: technical because of the maturity of the technology [1], economical due to a relevant cost reduction [2] and social because of the citizen involvement on decarbonising its electrical consumption [3].

The traditional operation of radial distribution systems cannot be maintained in case of a very high RES penetration because the design of these systems has been done to cope with power flows from primary and secondary substations to the final users [4]. The problems that RES may create have been profusely described in the specialised literature [5]: higher simultaneity coefficients, reverse power flows, nodal voltages out of control, power quality deterioration, increase of short-circuit power, etc. These technical problems can be released using conventional network reinforcement strategies ranging from increasing the cross-section of existing lines to installing new lines and/or power transformers. However, it has to be questioned whether this is the best solution taking into account the increase of cost and connection time [6] as well as the spare capacity of the new assets over a large number of hours per year [7]. Therefore, new alternatives must be explored to overcome the shortcomings related to this *Fit & Forget* approach.

Several active network operation approaches have been recently proposed, which can be classified according to the following characteristics: the control assets used to optimise the network operation, the applied control algorithms and the testing procedure used to validate their performance.

Control assets. Regarding to the first issue, HV/MV transformers equipped with on-load tap changers (OLTCs) and step voltage regulators have been proposed in [8]. In addition, RES may also contribute to the voltage regulation and congestion management by using adequate reactive power injections [9–11] or even resorting to curtailment [12]. However, it is important to mention that most of the active operation approaches consider several control assets that are managed in a coordinated manner: HV/MV OLTC and RES [13–15]; HV/MV OLTC and energy storage systems [16,17]; HV/MV OLTC, RES reactive power injection and DC links [18].

Control methodology. The active management solutions can be broadly classified into centralised, distributed and local methodologies. The centralised approaches rely on a control centre in charge of computing the optimal setpoints for all the control assets considering the available network measurements [19]. Local approaches are just the opposite because the actions taken by the control assets are calculated based on local measurements [9,11,14,20]. With this regard, distributed methods can be considered a compromise solution between the previous alternatives with several advantages related to robustness and scalability [21,22].

Testing methodology. The methodologies are usually validated by applying steady-state simulations considering daily profiles of load and generation. However, it can be also found other proposals using real-time digital simulators [21] and power hardware-in-the-loop platforms [17].

This paper tests a centralised control of active assets to manage MV distribution networks with a massive RES penetration. An Optimal Power Flow (OPF) is used to compute the optimal setpoints for three kinds of control assets: 1) HV/MV-transformer OLTCs; 2) RES reactive power injections and 3) active and reactive power through DC link meshing radial feeders. A high-RES but realistic load/generation scenario is analysed considering some test cases involving different sets of control assets with the aim of evaluating their performance. These test cases are implemented in a laboratory scaled-down active distribution network including hardware devices, controllers, communication infrastructure and a real-time monitoring system [23]. This testbed can be used to evaluate practical implementation issues of any centralised control algorithm related to the applied control strategy, the required data field, the communication systems, etc. as a previous step of its field deployment. Therefore, the main contribution of this paper is the experimental validation of the centralised controller proposed in [18] within an updated version of the testbed described in [23] in which an OLTC transformer and a DC link has been incorporated.

The paper is organised as follows. In section 2, a description of the centralised control to manage high-RES active distribution networks is presented. In section 3, the benchmark distribution network is described in detail including its main components and how they have been represented in the laboratory scaled-down testing platform. Section 4 depicts and analyses the system performance in different test cases comparing them in a quantitative manner by means of key performance indices (KPIs). Finally, Section 5 closes with the main conclusions.

2. Proposed centralised control

Smart Grids are characterized by an extensive measurement, automation and communication infrastructures which allows a safe and optimized network operation taken advantage of centralized Advanced Distribution Management Systems (ADMS). The main role of any ADMS in this environment is to concentrate all the field data to extract the required information about the network status and, in those cases where control assets are in operation, compute and send the required control actions optimizing the network operation according to a given criterium.

Figure 1 depicts this centralised control approach. First, the smart meters are in charge of measuring the load demanded by industrial (P_{il} and Q_{il}) and residential (P_{hl} and Q_{hl}) clients. In

Preprints (www.preprints.org) | NOT PEER-REVIEWED | Posted: 2 November 2018 doi:10.20944/preprints201811.0031.v1

Peer-reviewed version available at Energies 2018, 11, 3364; doi:10.3390/en11123364

addition, the RES active power injections such as the wind turbine (WT) and photovoltaic (PV) plants, P_{wt} and P_{pv} respectively, are also measured.

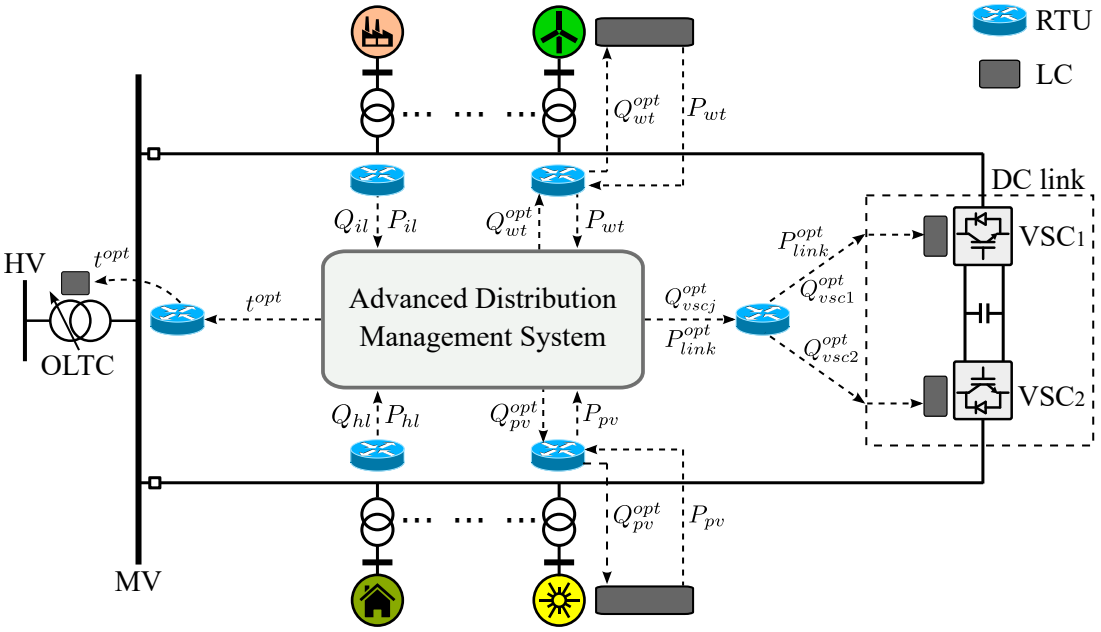

Figure 1. Architecture of a centralised control of an active distribution system.

All this field data are sent to the ADMS by means of Remote Terminal Units (RTUs) at regular time intervals (typically 5 to 15 minutes). Considering all this information, it is possible to compute setpoints for the installed control assets using an OPF to optimize any technical or economic objective. This paper considers, on the one hand, the following control assets:

- RES, which can regulate their reactive power injections Q_{wt}^{opt} and Q_{pv}^{opt}.
- Transformer OLTCs, which can adjust the tap position t^{opt}.
- DC link, which is composed of two Voltage Source Converters (VSCs) in back-to-back topology connecting two radial feeders. This device can regulate the active power flow between the feeders, P_{link}^{opt}, and two independent reactive power injections, $Q_{vsc\,j}^{opt}$. It is important to point out that the DC link is an interesting control asset with proven capability of reducing the network active power losses, maximizing the penetration of RES, improving the network voltage profiles and avoiding branch saturations [18],[24].

On the other hand, the selected OPF objective is to minimize the active power losses of the system, to take advantage of the already available control assets to optimise the operation of the distribution grid, which leads to the following formulation:

$$\min_{\mathbf{x}} P_{\text{loss}}(\mathbf{x}, \mathbf{y}), \tag{1}$$

where $\mathbf{x}$ is the set of control variables (P_{link}^{opt}, $Q_{vsc\,j}^{opt}$, $Q_{wt,pv}^{opt}$, t^{opt}) and $\mathbf{y}$ is the set of load and generation power injections for a given time interval (P_{il}, Q_{il}, P_{hl}, Q_{hl}, P_{wt}, P_{pv}).

The optimization problem is completed including the relevant constraints. First, the network operational limits have to be considered. The voltages and currents of the sets of buses, $\mathcal{N}$,

and branches, $\mathcal{B}$, have to be within the regulatory boundaries, $[V_i^{min}, V_i^{max}]$, and below the cable ampacities, I_b^{max}, respectively as stated in (2) and (3):

$$V_i^{min} \leq V_i \leq V_i^{max} \quad \forall i \in \mathcal{N}, \tag{2}$$

$$0 \leq I_b \leq I_b^{max} \quad \forall b \in \mathcal{B}. \tag{3}$$

Second, the OLTC tap has to be within the limits as well as the apparent power of RES and DC-link VSCs have to be below their rated capability, according to (4)-(6):

$$t^{min} \leq t^{opt} \leq t^{max}, \tag{4}$$

$$S_{pv,wt} \leq S_{pv,wt}^{rat}, \tag{5}$$

$$S_{DClink} \leq S_{DClink}^{rat}. \tag{6}$$

Finally, other constraints which are included in the OPF are the active and reactive bus power balances and the power constraints modelling the DC link behaviour which can be found in [24].

3. Laboratory testing platform

The objective of the laboratory testing platform is to faithfully represent the real behaviour of an active distribution system including all its components to asses the performance of the centralised control strategy outlined in section 2. In this way, the testing platform has been built based on the MV benchmark distribution network proposed by CIGRE Task Force C06.04.02 devoted to study the RES integration in MV networks [25]. The main reasons that have motivated the selection of this system are detailed below:

- First, this network is based on an actual MV German distribution system fulfilling the proposed objective of the laboratory testing platform described above.
- Second, an important RES penetration is integrated into the network.
- Third, all the network data including topology, parameters of lines and cables, loads, RES and their corresponding daily load/generation curves are available and well documented.
- Fourth, the benchmark network includes a DC link, a key component of future active distribution system with high RES penetration.

The next subsections present the MV benchmark distribution system and its scaled-down version built in the laboratory for testing purposes, including the implemented control scheme and the communication infrastructure designed to operate the system as a flexible platform to evaluate the benefits of active distribution networks.

3.1. MV benchmark distribution network

The one-line diagram of the benchmark distribution system is shown in Figure 2 which is composed of two radial subsystems departing from a primary substation where a 20 MVA 110/20 kV transformer is installed equipped with an OLTC. The total network comprises 14 buses grouped in two radial feeders: 11 buses for subsystem 1 and 3 buses for subsystem 2. The total line length of subsystem 1 is about 15 km while subsystem 2 is just 8 km. In addition, different types of loads, involving industrial and domestic customers, as well as a large amount of RES are connected into the different buses. In spite of [25] considers different types of RES, this work exclusively includes PV and WT plants because its current maturity foreseen their massive deployment in the next years. In addition, the benchmark network includes a DC link used to connect both radial subsystems between nodes N8 and N14.

The 24-hour profiles of the total loads and RES of subsystem 1 and 2 are depicted in Figure 3. It is interesting to point out that the subsystem 1 is more loaded than subsystem 2. Moreover, most RES are located within subsystem 1 which partially compensate its higher load with this local generation.

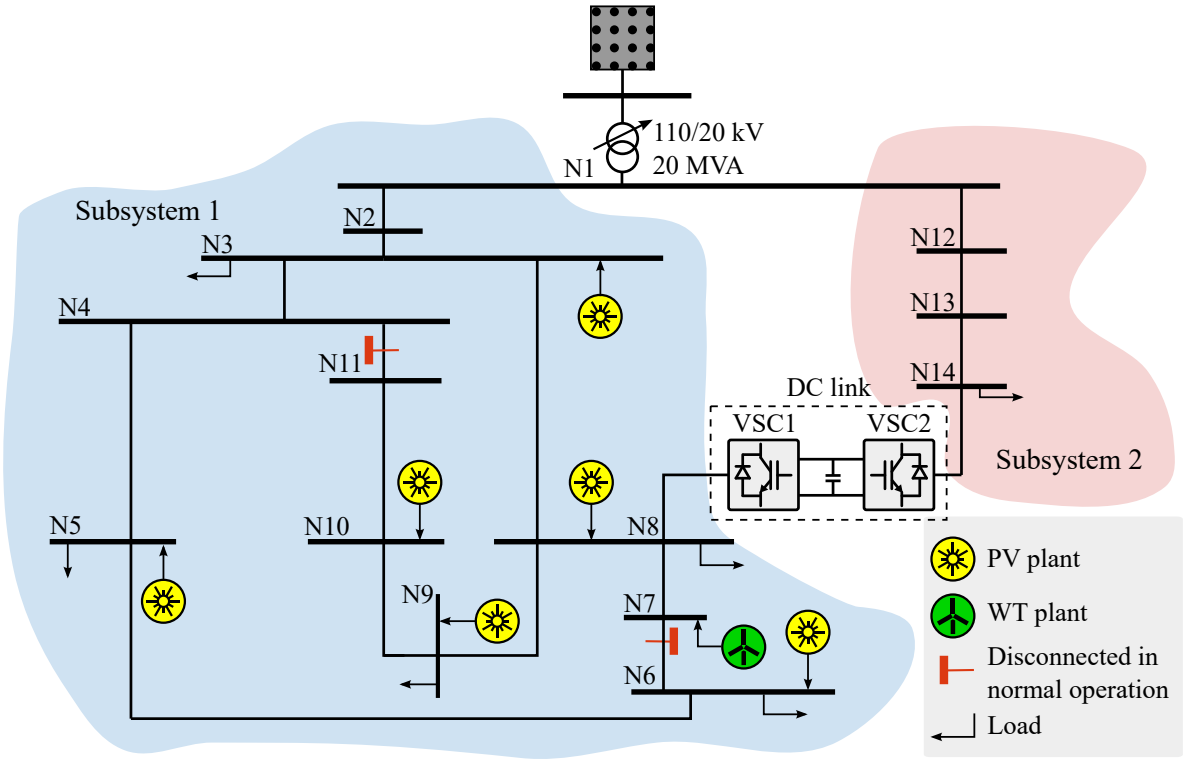

Figure 2. The MV benchmark distribution network proposed by the CIGRE Task Force C06.04.02.

It is also worth noting that, in order to analyse a case with a massive RES penetration, the generation has been multiplied by 4 and 400 in the case of the WT and PV plants respectively with respect to the scenario described in [25].

3.2. *Laboratory scaled-down distribution network*

This subsection provides a brief outline of the components and functionalities of the scaled-down testbed used to validate the benefits of the centralised controller. Basically, this hardware test rig, depicted in Figure 4, is a three-phase scaled-down representation, 400 V and 100 kVA, of the MV benchmark network analysed in subsection 3.1 which is composed of the following components:

- Distribution network branches. The electrical lines of both scaled-down subsystems have been represented using a lumped parameter model comprising the series resistor and reactor. The design considers original line R/X ratios and lengths to obtain per unit voltage drops similar to those produced in the actual system.
- Omnimode Load Emulators (OLEs). This is the building block responsible for representing any load, generator or a combination of them connected to any network node. Basically, each OLE is a VSC with a local controller (LC) whose AC and DC sides are connected to a scaled-down network node and a common DC bus respectively as shown in Figure 4. Note that all the OLEs share a common DC bus which is regulated by an extra balancing VSC. This is directly connected to the LV laboratory network by its AC side providing the net active power required by OLEs: $\sum P_i$. In this way, each OLE may absorb/inject (load/generator) any active power into the AC scaled-down distribution system within the technical constraints imposed by the VSCs: 20 kVA for individual OLEs and 100 kVA for the balancing VSC. The OLEs are connected to the following nodes: N3, N5, N6, N7, N8, N9, N10 (subsytem 1) and N14 (subsystem 2). The active and reactive power references to the OLEs are set by a Signal Management System (SMS) which will be detailed in the next subsection.

Preprints (www.preprints.org) | NOT PEER-REVIEWED | Posted: 2 November 2018 doi:10.20944/preprints201811.0031.v1

Peer-reviewed version available at Energies 2018, 11, 3364; doi:10.3390/en11123364

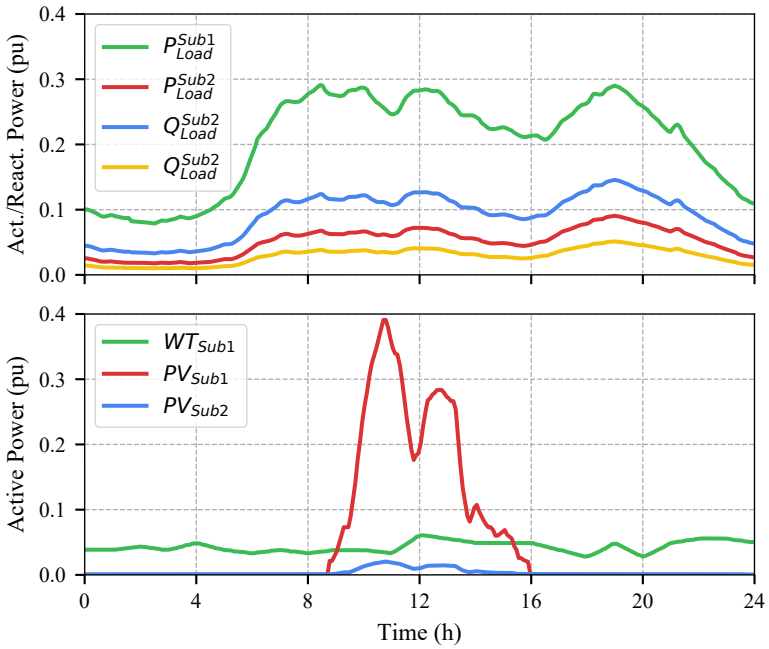

Figure 3. Top: Daily profile of the total load in subsystems 1 and 2; Bottom: Daily profile of the total WT and PV generation in subsystems 1 and 2.

A comprehensive description of this scaled-down system can be found in [23]. In addition, two new elements have been incorporated with the aim of integrating additional active control resources:

- Transformer with OLTC. The underlying idea is to represent the HV/MV transformers within the primary substations which are equipped with OLTCs to regulate the MV voltage. The transformer used for this purpose is a 400 V±5%/400 V, 100 kVA equipped with a thyristor-based tap changer as shown in Figure 4.
- DC link. This DC link, originally included in the benchmark distribution system [26], has been incorporated between N8 and N14 as a suitable device to maximise the RES penetration as stated previously. In spite of several topologies can be used to create a flexible loop between radially operated feeders [27], the DC link is based on a conventional back-to-back VSCs rated to 400 V and 10 kVA. Note that the DC bus of the DC link is totally independent of the one shared by the OLEs and balancing VSC.

The optimal setpoints for these two control assets are also managed by the SMS in a similar manner than the OLE power references.

3.3. Control scheme and communication system

The control system is a two-level hierarchical structure as shown in Figure 5. The first control level comprises the SMS which is in charge of sending the references to the hardware components whereas the second control level is composed of several LCs attached to the hardware devices (OLEs, DC link and OLTC) being responsible of tracking these references.

The SMS performs two tasks in a sequential manner which can be summarised as follows:

- Off-line tasks. They are carried out by a Host PC and mainly consist on the configuration of the setpoint profiles. The OLE active and reactive daily power curves ($P_i^\star$, $Q_i^\star$) are defined through two tools developed into the Host PC [23]. Once these profiles have been determined, the daily setpoints of the DC link, P^{opt}_{link} and Q^{opt}_{vscj}, the reactive power injected by the RES, $Q^{opt}_{wt,pv}$, and the optimal OLTC tap position, t^{opt}, are automatically computed by the OPF described in section 2.

Preprints (www.preprints.org) | NOT PEER-REVIEWED | Posted: 2 November 2018 doi:10.20944/preprints201811.0031.v1

Peer-reviewed version available at Energies 2018, 11, 3364; doi:10.3390/en11123364

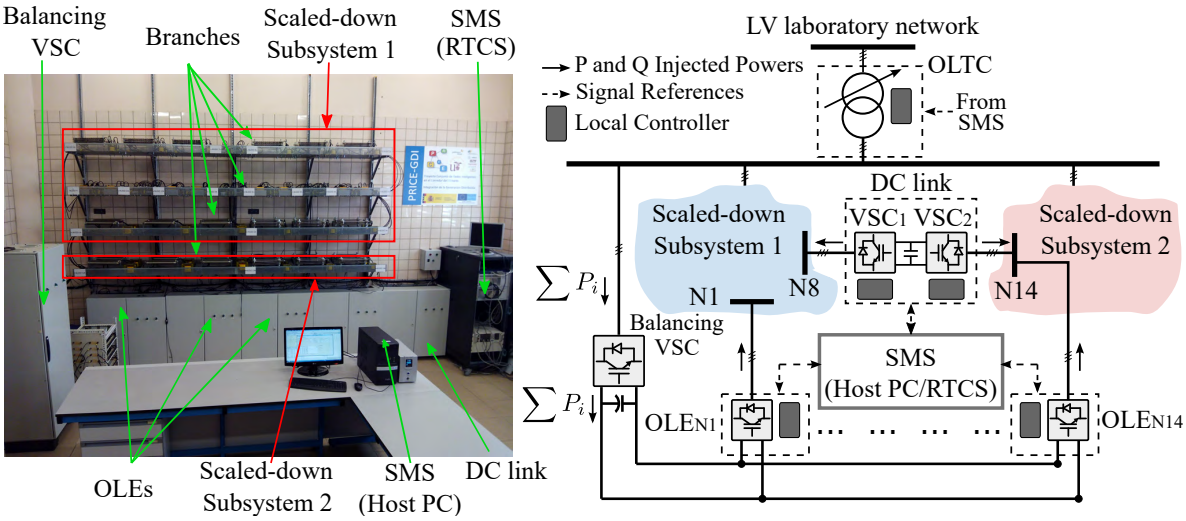

Figure 4. Left: Layout of laboratory testbed. Right: One-line diagram of the updated testbed including the DC link and the transformer with OLTC.

Finally, all these data are compiled and uploaded to the Real-Time Control System (RTCS) for its real-time operation.

- On-line tasks. These are executed by the RTCS which is responsible for two undertakings. On the one hand, the RTCS is in charge of sending the setpoints to the second control level, composed of the LCs attached to each hardware controllable component, during the on-line operation according to the profiles previously determined in the off-line tasks. On the other hand, the RTCS receives measurements from each each LC attached to the OLEs (V_i, P_i and Q_i), DC-link VSCs (V_{vscj},P_{link} and Q_{vscj}) and tap position of the transformer OLTC (t^{opt}). After processing this information, it provides a real-time monitoring of the system which is displayed in the Host PC.

The second level of the control system is composed of the LCs of each OLE, DC-link VSCs and transformer OLTC which are implemented in Digital Signal Processors. These are in charge of tracking the setpoints sent by the RTCS during the on-line operation.

The communication infrastructure required to connect the centralised RTCS with the LCs is based on a 100 MBs Ethernet LAN network as physical layer being implemented a communication protocol based on UDP/IP. Finally, an asynchronous communication protocol TCP/IP is implemented between Host PC and the RTCS.

4. Experimental assessment of the proposed centralised control

This section is devoted to analyse the performance of the centralised control on the scaled-down system under different test cases. These will be evaluated through KPIs to quantify the influence of the considered control assets in high-RES active distribution networks.

4.1. Test Cases Definition

Table 1 shows the definition of the designed test cases. The first case C1 corresponds to a base case where no control assets are included in the distribution system and the OLTC is set in the central tap position. The subsequent test cases add the control assets in the centralised control in an incremental manner. In this way, it should be possible to quantify the impact that each control asset has in the system performance.

Preprints (www.preprints.org) | NOT PEER-REVIEWED | Posted: 2 November 2018 doi:10.20944/preprints201811.0031.v1

Peer-reviewed version available at Energies 2018, 11, 3364; doi:10.3390/en11123364

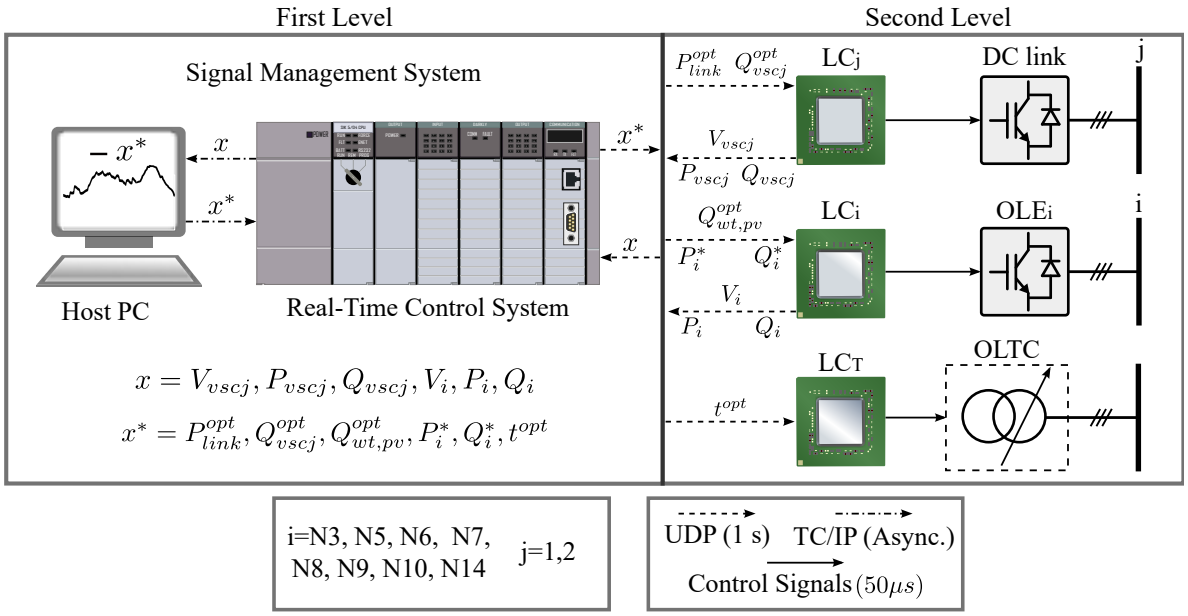

Figure 5. General control scheme of the testing environment.

Table 1. Definition of test cases.

Control assets	C1	C2	C3	C4
OLTC		•	•	•
RES reactive power			•	•
DC link				•

4.2. Definition of KPIs

The following KPIs have been selected to analyse the performance of the centralised control and its related control assets:

- Daily energy losses ($E_{loss}/\Delta E_{loss}$). This KPI measures the daily active energy losses in kWh/day, E_{loss}, and the percentage of loss reduction with respect to the base case C1, ΔE_{loss}.
- Voltage violation (T_{vv}). This KPI evaluates the percentage of the time of the day in which the nodal voltages are outside the technical limits [0.95-1.05 pu].
- Variation of nodal voltages (ΔV). This index provides a global measurement of the daily voltage variations at the nodes of the network. It is computed as the average value of the difference between the maximum and minimum nodal voltages measured in pu,

$$\Delta V = \frac{\sum_{\mathcal{N}}(V_i^{max} - V_i^{min})}{Ni}, \tag{7}$$

where Ni is the total number of the network nodes.

- OLTC operation (N_{OLTC}). This KPI shows the number of OLTC operations during the 24-hours testing period.
- RES reactive power injection (Q_{RES}). This index provides a global measurement of the RES collaboration to the network reactive power support. It is computed dividing the average value of the reactive power injected by the RES during the 24 hours by the total number of RES,

$$Q_{RES} = \frac{\sum_{i,t} Q_{RES_{i,t}}}{N_t \times N_{RES}}, \tag{8}$$

where $Q_{RES_{i,t}}$ is the reactive power injected by RES_i in period t, N_{RES} is the number of RES in the network and N_t is the number of time periods considered during the 24 hours.

- DC Link load (SL_{link}). This evaluates the state of load of the DC link during the day and it is computed as:

$$SL_{link} = \frac{\sum_{j,t} S_{vscj,t}}{N_t \times S_{DClink}}, \tag{9}$$

where S_{vscj} is the apparent power of each VSC and S_{DClink} is the rated power of the DC link.

- Transformer load (T_L). It represents the daily average load of the transformer as a percentage of its rated power, which can be computed as:

$$T_L = \frac{\sum_t S_t^T}{N_t \times S_N}, \tag{10}$$

where S^T is the apparent power through the transformer and S_N is the rated power of the transformer.

4.3. Experimental Results

The objective function proposed for the operation of high-RES active distribution networks is based on an operation with minimal technical losses. This section is devoted to evaluate the previously described test cases analysing the following electrical magnitudes: power losses, nodal voltages and current circulating at the primary substation transformer. In addition, the previously defined KPIs allow to quantify in a comprehensive manner the key magnitudes to assess the performance of the proposed control.

Table 2 shows the E_{loss} for the studied test cases and the loss reduction with respect to the base case C1, ΔE_{loss}, when the load and generation daily profiles presented in subsection 3 are implemented into the testing platform. In the laboratory testbed, the 24-hour profiles are scaled to last 48 minutes and reduce the duration of the tests.

Table 2. KPIs used for the evaluation of the test cases.

	C1	C2	C3	C4
$E_{loss}/\Delta E_{loss}$ (kWh/%)	58.37/–	55.69/4.58	50.17/16.33	46.47/25.59
Q_{RES} (pu)	–	–	0.117	0.095
T_{vv} (%)	38.69	0	0	0
N_{OLTC}	0	2	4	2
ΔV (pu)	0.087	0.061	0.058	0.042
T_L (%)	24.95	24.43	20.62	20.20

C1 presents the greatest daily power losses as no control assets are operating to act on the voltages and power flows that help to reduce the system losses. The introduction of the OLTC operation in C2 reduces energy losses by almost a 5 %. The OLTC setpoint is computed in the OPF whose objective function is to reduce the total power losses in the network. Therefore, the tap is established in -5% position in order to increase the nodal voltages and achieve the intended objective.

In the test case C3, the RES reactive power capability is also included in the control. Now, the daily energy losses are reduced more than 15% with respect to C1. This occurs because the RES are able to provide reactive power to the system. Figure 6 shows the RES reactive power injected at nodes N3 and N8 with respect to their rated power for the test cases C3 and C4. This is represented using violin plots which allow to visualise the distribution of any magnitude as well as its range of variation and frequency of occurrence. Note that most of the time, which corresponds to the wider part of the violin plot, the RES are injecting reactive power corresponding to 20% of their rated power. This high RES reactive power injection is used to feed part of the reactive power demanded by the loads, thus avoiding the need to be supplied from the primary substation. as shown in Figure 7. Note that the

reactive power supplied from the primary substation in C3 is lower than 0.05 pu during the 24 hours, helping to reduce the energy losses.

The DC link integration in C4 further reduces the energy losses up to a 25% with respect to C1, as shown in Table 2. This device injects reactive power at the interconnected nodes N8 and N14 by means of VSC1 and VSC2 respectively during the 24 hours as depicted in Figure 8. This power, added to the RES reactive power, leads to an almost zero reactive power supplied from the primary substation, as shown in Figure 7. In this way, the energy losses are reduced with respect to C3. An additional effect on the RES reactive power injections can be observed. In C4, the RES do not to have to inject as much reactive power as in C3, as can be observed in Figure 6, becoming even zero in some nodes like N8. This effect is quantified in a global manner with Q_{RES} collected in Table 2 where lower values for this KPI in C4 with respect to those in C3 can be appreciated. It is also worth noting that the DC link also controls the active power transferred from subsystem 1 to subsystem 2, as shown in Figure 8. Outside the period of high injection of RES active power (0-10 h and 13-0 h), the DC link absorbs active power from N14 and injects it into N8. This means that part of the load from subsystem 1 is powered by subsystem 2 which is less loaded and with shorter branches, helping to reduce the total power losses of the system. Conversely, within the hours of high RES active power injection, the active power flow is inverted in the DC link: VSC1 absorbs active power from subsystem 1 and it is injected by the VSC2 to subsystem 2. In this way, part of the power generated by RES in subsystem 1 is transferred to feed the loads in subsystem 2. Therefore, this active power is not supplied by the primary substation thus reducing the current in this system and the energy losses.

Finally, note that the DC-link state of load, SL_{link}, during the day is 49.4%. This means that the DC link is used at half load and there is still a wide margin to take advantage of its flexibility of operation. For example, the RES penetration in subsystem 1 could increase and still be managed by the current DC link.

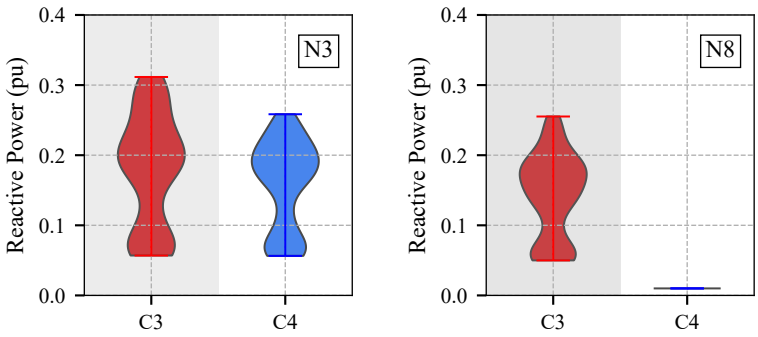

Figure 6. Violin plots of RES reactive power injections for the test cases C3 and C4 at nodes N3 and N8.

Figure 9 shows the 24-hour nodal voltages at nodes N3, N6, N8 and N14 for the different test cases. These buses have been selected to represent the behaviour of nodes nearby (N3) and far from (N6) the primary substation. In addition, nodes N8 and N14 have been also included because they are the connection points of the DC link. The analysis of Figure 9 reveals that undervoltage situations, voltages below 0.95 pu, exclusively occur in the base case C1 due to the lack of control assets operating in the network. This situation leads to very high T_{vv} value in C1, as shown in Table 2. These voltage violations are more severe at nodes N6 and N8 corresponding to subsystem 1 because of two reasons. First, subsystem 1 is more loaded than subsystem 2, as depicted in Figure 3, especially during the hours without RES generation. This causes greater current flows and, consequently, greater voltage drops along the lines. This effect is especially significant around 8 and 20 hours when the RES generation is almost zero and the demand is peaking.

Preprints (www.preprints.org) | NOT PEER-REVIEWED | Posted: 2 November 2018 doi:10.20944/preprints201811.0031.v1

Peer-reviewed version available at Energies 2018, 11, 3364; doi:10.3390/en11123364

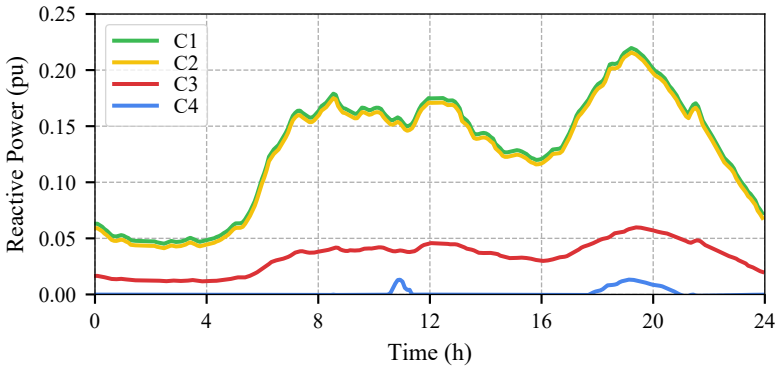

Figure 7. Reactive power flow through the primary substation for the test cases C1-C4.

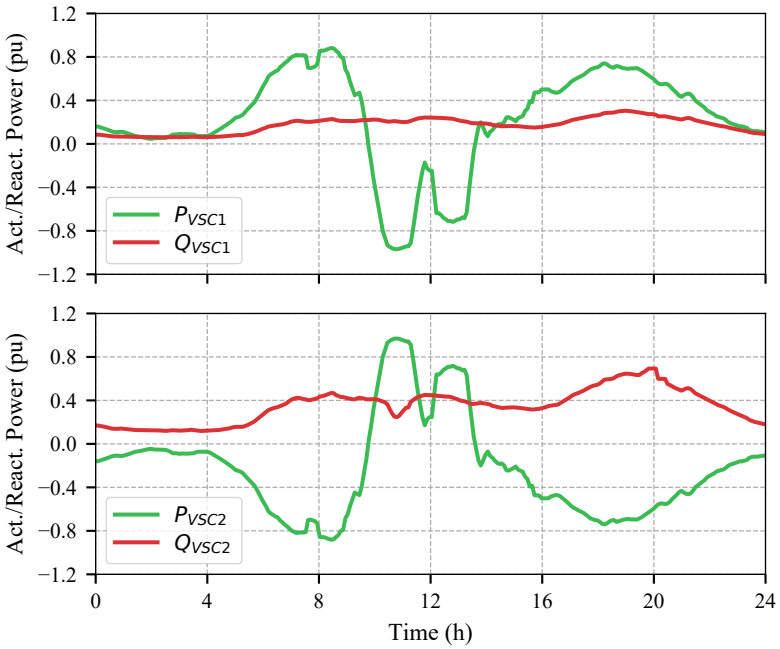

Figure 8. DC link active and reactive power daily profiles.

The introduction of the OLTC in C2 pushes the voltages within the ± 0.05 pu regulatory band around the rated voltage and, consequently, voltage violations are eliminated, as illustrated by its T_{vv}. In C2, the tap is established in the -5% position during most of the day. However, and according to the information provided in Table 2, two OLTC operations N_{OLTC} (from -5% to 0% position) over the 24-hours period are required to maintain the voltages within the limits. These changes occur around 11 and 13 hours when RES generation is maximum, as shown in Figure 3, and the network voltages are excessively high. The range of variation of nodal voltages ΔV is significantly reduced with respect to C1 as shown in Table 2. This effect can also be observed in Figure 9 where the violin plots are shortened, concentrating the nodal voltages within a narrower band. This trend is maintained in C3 due to the contribution of RES to regulate the voltage with reactive power injections. In addition, it can be seen that also the average voltage of nodes N3, N6 and N8 from subsystem 1 increase due to the local effect of the reactive power injections. As a consequence, additional OLTC changes N_{OLTC} (from -5% to 0% position) are required to maintain the voltages within the technical limits. This longer time of the tap within the 0% position causes lower voltages within subsystem 2 as can be observed for the node N14 in Figure 9.

Preprints (www.preprints.org) | NOT PEER-REVIEWED | Posted: 2 November 2018 doi:10.20944/preprints201811.0031.v1

Peer-reviewed version available at Energies 2018, 11, 3364; doi:10.3390/en11123364

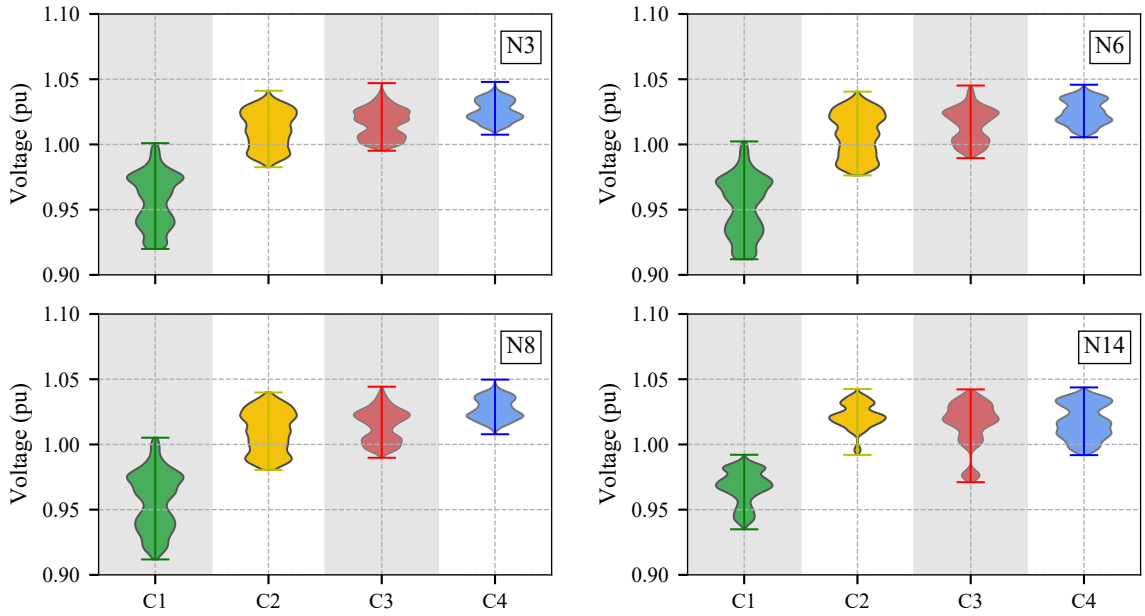

Figure 9. Violin plots of nodal voltages for test cases C1 to C4 at nodes N3, N6, N8 and N14.

C4 incorporates the operation of the DC link between nodes N8 and N14 allowing to inject additional reactive power in these nodes and active power transfer between both subsystems. This leads to the minimum range of variation of the nodal voltages ΔV and the maximum value of these in all the test cases. In fact, in C4 the voltages oscillate in a range between 1 and 1.05 pu over the 24-hour period.

Figure 10 shows the daily evolution of the current circulating through the primary substation transformer for the studied test cases. This current is reduced as the number of control assets is increased. The analysis of C4 reveals that during some periods the current is almost zero. This means that the RES generation, adequately managed by the control assets, is enough to operate the system without the need of supplementary power from the primary substation. Finally, it is worth noting that the state of load of the transformer T_L is also progressively reduced in the subsequent test cases, as shown in Table 2. As a consequence, the benefits for the distribution system are clear in this respect: reduction of transformer losses, increment of useful life and increase of the system loadability which allows to defer new investment in power assets.

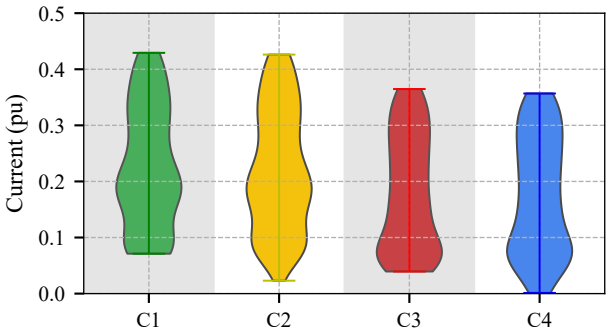

Figure 10. Violin plots of MV current at primary substation transformer for test cases C1 to C4.

5. Conclusions

This paper has assessed in an experimental manner the benefits of a centralised controller for active distribution networks with high-RES penetration. The paper proposes to optimise the operation of the system by minimising the active power losses through an OPF with the following control assets: (i) transformers equipped with OLTC; (ii) RES reactive power injections and (iii) DC links. The assessment of the proposed centralised controlled has been done in a laboratory scaled-down version of the MV network proposed by the CIGRE Task Force C06.04.02. This testing platform has been described including its main components and functionalities as well as the new control assets (transformer OLTC and DC link) which have been incorporated with respect to a previous version to improve its testing capabilities. The paper has defined a comprehensive design of the testing procedure including some test cases involving different control assets and a set of KPIs to deal with a quantintative comparison of performance. The obtained results has revealed that a centralised control of high-RES active distribution networks may improve their operation. As a matter of fact, this improvement is of significance in case of control assets which are commonly present in distribution networks, i.e. transformers with OLTCs and RES reactive power injections. Moreover, this enhancement could be even larger if not common but matured enough technologies, like DC links, are progressively introduced in the distribution business. This will increase the RES network hosting capacity contributing to the decarbonization of our society.

Acknowledgments: The authors would like to acknowledge the financial support of the Spanish Ministry of Economy and Competitiveness under Grants ENE2015-69597-R, PCIN-2015-043 and ENE2017-84813-R.

Author Contributions: F.P.G.L reviewed the state of the art, designed the test cases and the control algorithms, was responsible for laboratory testing and discussion of the obtained results and wrote part of the paper; M.B.V. supported the laboratory testing, contributed to the analysis of the results and wrote part of the paper; A.M.M. was responsible of the OPF definition, contributed to the analysis of results and wrote part of the paper; J.M.M.O. defined the KPIs, contributed to the the discussion of results and wrote part of the paper; J.L.M.R. supported the OPF definition and practical implementation issues and discussed to the results of the paper.

Conflicts of Interest: The authors declare no conflict of interest.

Abbreviations

The following abbreviations are used in this manuscript:

ADMS: Advanced Distribution Management System
KPI: Keys Performance Index
LC: Local Controller
LV: Low Voltage
MV: Medium Voltage
OLE: Omnimode Load Emulator
OPF: Optimal Power Flow
OLTC: On-Load Tap Changer
PV: Photovoltaic
RES: Renewable Energy Sources
RTCS: Real-Time Control System
RTU: Remote Terminal Unit
SMS: Signal Management System
VSC: Voltage Source Converter
WT: Wind Turbine

Bibliography

1. Guerrero, J.M.; Blaabjerg, F.; Zhelev, T.; Hemmes, K.; Monmasson, E.; Jemei, S.; Comech, M.P.; Granadino, R.; Frau, J.I. Distributed Generation: Toward a New Energy Paradigm. *IEEE Industrial Electronics Magazine* **2010**, *4*, 52–64.
2. Distributed Generation System Characteristics and Costs in the Buildings Sector. Technical report, U.S. Energy Information Administration, 2013.
3. Pérez-Arriaga, I.; Knittel, C. Utility of the Future. An MIT Energy Initiative response. Technical report, Massachusetts Institute of Technology, 2016.
4. Power Distribution Planning Reference Book, Second Edition, 2004.
5. Barker, P.P.; Mello, R.W.D. Determining the impact of distributed generation on power systems. I. Radial distribution systems. 2000 Power Engineering Society Summer Meeting (Cat. No.00CH37134), 2000, Vol. 3, pp. 1645–1656 vol. 3.
6. Walling, R.A.; Saint, R.; Dugan, R.C.; Burke, J.; Kojovic, L.A. Summary of Distributed Resources Impact on Power Delivery Systems. *IEEE Transactions on Power Delivery* **2008**, *23*, 1636–1644.
7. Assessing the impact of low carbon technologies on Great Britain's power distribution networks, 2012.
8. Elkhatib, M.E.; El-Shatshat, R.; Salama, M.M.A. Novel Coordinated Voltage Control for Smart Distribution Networks With DG. *IEEE Transactions on Smart Grid* **2011**, *2*, 598–605.
9. Molina-García, A.; Mastromauro, R.A.; García-Sánchez, T.; Pugliese, S.; Liserre, M.; Stasi, S. Reactive Power Flow Control for PV Inverters Voltage Support in LV Distribution Networks. *IEEE Transactions on Smart Grid* **2017**, *8*, 447–456.
10. Calderaro, V.; Galdi, V.; Lamberti, F.; Piccolo, A. A Smart Strategy for Voltage Control Ancillary Service in Distribution Networks. *IEEE Transactions on Power Systems* **2015**, *30*, 494–502.
11. Karagiannopoulos, S.; Aristidou, P.; Hug, G. Hybrid approach for planning and operating active distribution grids. *Transmission Distribution IET Generation* **2017**, *11*, 685–695.
12. Ueda, Y.; Kurokawa, K.; Tanabe, T.; Kitamura, K.; Sugihara, H. Analysis Results of Output Power Loss Due to the Grid Voltage Rise in Grid-Connected Photovoltaic Power Generation Systems. *IEEE Transactions on Industrial Electronics* **2008**, *55*, 2744–2751.
13. Alnaser, S.W.; Ochoa, L.F. Advanced Network Management Systems: A Risk-Based AC OPF Approach. *IEEE Transactions on Power Systems* **2015**, *30*, 409–418.
14. Kryonidis, G.C.; Demoulias, C.S.; Papagiannis, G.K. A Nearly Decentralized Voltage Regulation Algorithm for Loss Minimization in Radial MV Networks With High DG Penetration. *IEEE Transactions on Sustainable Energy* **2016**, *7*, 1430–1439.
15. Kolenc, M.; Papič, I.; Blažič, B. Minimization of losses in smart grids using coordinated voltage control. *Energies* **2012**, *5*, 3768–3787. Cited By :11.
16. Alnaser, S.W.; Ochoa, L.F. Hybrid controller of energy storage and renewable DG for congestion management. 2012 IEEE Power and Energy Society General Meeting, 2012, pp. 1–8.
17. Liu, X.; Aichhorn, A.; Liu, L.; Li, H. Coordinated Control of Distributed Energy Storage System With Tap Changer Transformers for Voltage Rise Mitigation Under High Photovoltaic Penetration. *IEEE Transactions on Smart Grid* **2012**, *3*, 897–906.
18. Barragan-Villarejo, M.; Marano, A.; García-López, F.P.; Mauricio, J.M.; Maza-Ortega, J.M. Coordinated control of distributed energy resources and flexible links in active distribution networks. International Conference on Renewable Power Generation (RPG 2015), 2015, pp. 1–6.
19. Calderaro, V.; Galdi, V.; Lamberti, F.; Piccolo, A. A Smart Strategy for Voltage Control Ancillary Service in Distribution Networks. *IEEE Transactions on Power Systems* **2015**, *30*, 494–502.
20. Fazio, A.R.D.; Fusco, G.; Russo, M. Decentralized Control of Distributed Generation for Voltage Profile Optimization in Smart Feeders. *IEEE Transactions on Smart Grid* **2013**, *4*, 1586–1596.
21. Kulmala, A.; Alonso, M.; Repo, S.; Amaris, H.; Moreno, A.; Mehmedalic, J.; Al-Jassim, Z. Hierarchical and distributed control concept for distribution network congestion management. *Transmission Distribution IET Generation* **2017**, *11*, 665–675.
22. Almasalma, H.; Claeys, S.; Mikhaylov, K.; Haapola, J.; Pouttu, A.; Deconinck, G. Experimental Validation of Peer-to-Peer Distributed Voltage Control System. *Energies* **2018**, *11*, 1304.

23. Maza-Ortega, J.M.; Barragán-Villarejo, M.; García-López, F.d.P.; Jiménez, J.; Mauricio, J.M.; Alvarado-Barrios, L.; Gómez-Expósito, A. A Multi-Platform Lab for Teaching and Research in Active Distribution Networks. *IEEE Transactions on Power Systems* **2017**, *32*, 4861–4870.
24. Romero-Ramos, E.; Gómez-Expósito, A.; Marano-Marcolini, A.; Maza-Ortega, J.M.; Martínez-Ramos, J.L. Assessing the loadability of active distribution networks in the presence of DC controllable links. *IET Generation, Transmission & Distribution* **2011**, *5*, 1105.
25. Rudion, K.; Orths, A.; Styczynski, Z.A.; Strunz, K. Design of benchmark of medium voltage distribution network for investigation of DG integration. 2006 IEEE Power Engineering Society General Meeting, 2006, pp. 6 pp.–.
26. Benchmark Systems for Network Integration of Renewable and Distributed Energy Resources.
27. Maza-Ortega, J.m.; Gomez-Exposito, A.; Barragan-Villarejo, M.; Romero-Ramos, E.; Marano-Marcolini, A. Voltage source converter-based topologies to further integrate renewable energy sources in distribution systems. *IET Renewable Power Generation* **2012**, *6*, 435–445.